Small Systems of Nonlinear Oscillators

Matthew Grau
Department of Physics, California Institute of Technology, Pasadena, CA 91125, USA

Coupled oscillators are used to model systems such as arrays of lasers or detectors whose response is combined to increase signal strength. I investigated systems of two and three coupled nonlinear oscillators, focusing on two different models: One model includes only the phases of the oscillators, and the other includes both phases and amplitudes. The second model also incorporates features such as reactive (non-dissipative) force couplings and amplitude-dependent frequencies. I studied both models analytically to determine regions of synchronization, a phenomenon in which many oscillators lock their phase or frequency to a common equilibrium value, and then employed careful numerical simulations to verify the analytical calculations and extend the results to cases that were not analytically tractable. The result of the investigation of the amplitude model can be used to motivate the choice of parameter values (such as spread of intrinsic frequencies or coupling strength) of small systems of nanomechanical oscillators currently being designed in the M. Roukes laboratory at Caltech.

Keywords: synchronization, nonlinear oscillators, NEMS

Typically study of coupled oscillators is done on a continuous limit or on a handful. This is because the analysis of discrete oscillators becomes very difficult for even as few as five or six oscillators. In this paper, I study two models: a phase model with dissipative coupling between three oscillators and a model of two oscillators that includes more features, including amplitude dynamics, amplitude-dependent frequencies, and reactive (non-dissipative) coupling. The second model was motivated by an array of nano-electromechanical cantilevers currently being designed and fabricated by Michael Roukes' group at Caltech. I used a combination of analytics and numerical simulation (integration routines performed by python) during investigation. My results include a description of the behavior of the models across parameter space.

INTRODUCTION

Numerous physical systems can be modeled by interacting nonlinear oscillators [6]. An exciting quality of such systems is their ability to oscillate collectively at a common frequency or phase even when the individual oscillators have different intrinsic frequencies or initial phases. This phenomenon is known as *synchronization*. Small groups of oscillators are directly applicable to synchronizing systems, such as lasers that are coupled to increase power output [4], and nanomechanical oscillators, where synchronization to a common frequency can eliminate the inevitable frequency differences arising from imperfections in fabrication [3]. Understanding small numbers of coupled oscillators can be useful in the development of "renormalization group" methods to analyze very large systems (such as the synchronized flashing of fireflies [2]).

The general solution to a system of nonlinear oscillators can be very complicated. However, specific solutions can be obtained by taking the limit as the number of oscillators gets either very large or very small and then simplifying various aspects, such as assuming that only phase matters or assuming some symmetry, such as a coupling between oscillators that is all-to-all [5]. Previous work in this field has focused on the continuum limit of a very large number of oscillators and the limit of very small number of oscillators. In this project I investigate systems of two and three oscillators.

This paper is organized as follows. It's first half of this paper is devoted to a discussion of the phase model. First I analyze the phase model in its symmetric special case in which two of the three intrinsic frequencies are the same and a center oscillator coupled is to the other two end oscillators (which are each only coupled to the center). I then investigated how the dynamics is affected when this symmetry s broken. Finally, I examined what happens when each oscillator is coupled to each other oscillator. The second half of this paper discusses an amplitude model with reactive coupling and nonlinear frequency pulling. In this case, I consider systems of two coupled oscillators.

PHASE MODEL

A prototypical model of coupled phase oscillators is the Kuramoto model [1],

$$\dot{\theta}_m = \omega_m + \sum_{n=1}^{N} K_{n,m} \sin(\theta_n - \theta_m). \tag{1}$$

There are N total oscillators. The mth oscillator has phase θ_m, intrinsic frequency ω_m, and a coupling to the nth oscillator of strength $K_{n,m}$. The primary interesting attribute of this model arises from the fact that the coupling of oscillators is nonlinear due to the sin term. In this coupling only the relative phase of the oscillators is important.

While equation (1) is typically analyzed for arrays of oscillators that approach a continuum limit (for which N is very large), this model still has interesting behavior when describing a finite number of oscillators. Because the model is nonlinear, even $N = 5$ or $N = 6$ yields a system that is difficult to analyze (or even intractable). I accordingly consider $N = 3$.

Equal Intrinsic Frequencies

I further simplify the model by imposing $\omega_1 = \omega_3$ and $K_{1,3} = K_{3,1} = 0$. The restriction on the coupling yields a topology in which a center oscillator is coupled to two end oscillators that are not coupled to each other. I will refer to this as coupling on a "line." The alternative is that each oscillator is coupled to each other oscillator; this is called "all-to-all" coupling. Additionally, I only examined equal coupling strengths (all couplings are strength K), so that the equations of motion become

$$\begin{aligned} \dot{\theta}_1 &= \omega_1 + K \sin(\theta_2 - \theta_1), \\ \dot{\theta}_2 &= \omega_2 + K \sin(\theta_1 - \theta_2) + K \sin(\theta_2 - \theta_3), \\ \dot{\theta}_3 &= \omega_3 + K \sin(\theta_2 - \theta_3). \end{aligned} \tag{2}$$

I analyzed this system of equations by considering the two-oscillator system of the relative phases of each of the end oscillators with respect to the center oscillator. Define new variables for these relative phases, $\phi_1 \equiv \theta_2 - \theta_1$, $\phi_2 \equiv \theta_2 - \theta_3$, rescale time using $t \to t'K$, and introduce the parameter $\rho \equiv (\omega_2 - \omega_1)/K = (\omega_2 - \omega_3)/K$. This yields the two dimensional system

$$\begin{aligned} \dot{\phi}_1 &= \rho - 2\sin\phi_1 - \sin\phi_2 \\ \dot{\phi}_2 &= \rho - 2\sin\phi_2 - \sin\phi_1 \end{aligned} \tag{3}$$

The equilibria of (3) give conditions for frequency locking in (2). I obtained the equilibria $(\bar{\phi_1}, \bar{\phi_2})$ by finding the conditions for $\dot{\phi}_1 = \dot{\phi}_2 = 0$. This requires that $|\rho| \leq 3$. When $|\rho| < 3$ there are four equilibrium points, each of which satisfy $3\sin\bar{\phi} = \rho$. When $|\rho| = 3$, there is a single equilibrium at $sign(\rho)(\pi/2, \pi/2)$, as a bifurcation occurs for that parameter value.

For the of this paper I will only consider $\rho \geq 0$. When $\rho < 0$ the phase space can be reflected about each axis ($\phi_1' = -\phi_1$ and $\rho_2' = -\rho_2$). This reflected system has the same properties of the original system. Examining the stability of the equilibrium points by considering small perturbations around each point and ignoring second order terms to linearize the system shows that only one of the points is stable. There are also two are saddles and one source. The stable point is always located at $(\arcsin(\rho/3), \arcsin(\rho/3))$ (as shown in point A on Fig 1). The four equilibria are situated at the vertices of a square centered at $(\pi/2, \pi/2)$. A stable synchronized solution exists for $rho < 3$. When $\rho = 3$, the equilibrium eigenvalues all vanish.

The saddle points in the system give rise to some interesting behavior. For certain ranges of ρ, it is possible for the saddles to be connected by homoclinic orbits (when the stable manifold of one saddle connects to the unstable manifold of the same saddle). It is also possible for a heteroclinic orbit to exist (when the stable manifold of one saddle connects to the unstable manifold of the other). The homoclinic orbits of the saddles act as separatrices, dividing phase space into a region that contains equilibrium points and another that does not contain equilibrium points. These separatrices define the basin of attraction of the stable equilibrium, (see Fig. 1).

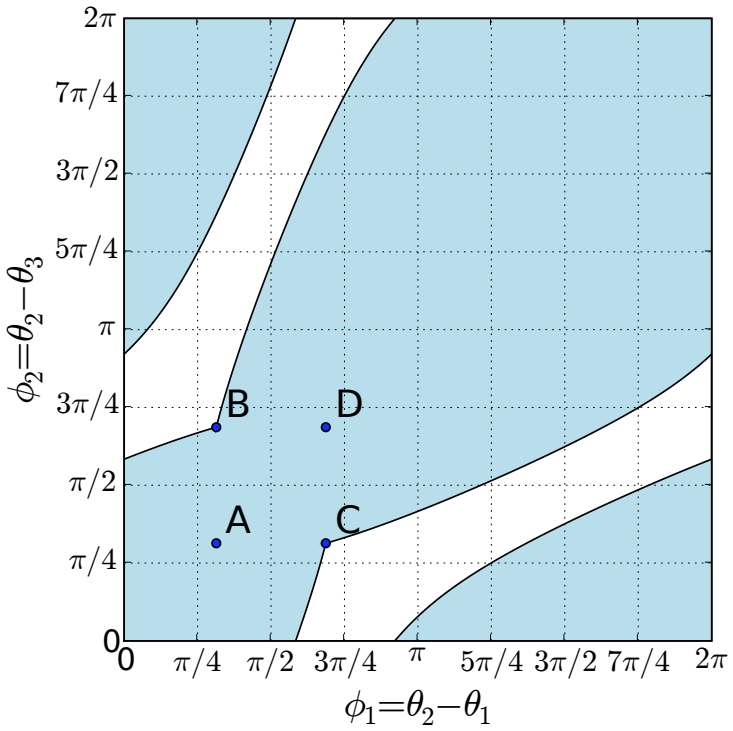

FIG. 1: [Color online] Phase portrait of equation (3) with $\rho = 5/2$. The shaded area is the basin of attraction of the stable equilibrium point (A). Also labeled in this figure are two saddle points (B) and (C) and an unstable node (D). The equilibria are located at the vertices of a square centered at $(\pi/2, \pi/2)$. Note that because the phase space is a torus, it follows that the points that lie on the left and right edges are the same, as are those that lie along the top and bottom edges. The two closed black curves separate the basin of attraction from the rest of phase space.

For some critical value ρ_c there is a heteroclinic orbit for $\rho = \rho_c$, but it does not divide the phase space. The saddles form homoclinic orbits for $\rho_c < \rho < 3$, and it is these homoclinic orbits that separate the phase space and define the basin of attraction. As ρ is increased from ρ_c to 3, the size of the basin of attraction relative to the entire space shrinks monotonically from 1 to 0 (see Fig. 3). Also as ρ changes from ρ_c to 3 the edges of the square whose vertices are defined by the location of the four equilibria shrinks in size from π to 0 as the equilibria converge to a point. By defining trapping regions I can prove rigorously that $\rho_c > 1/3$. By numerical simulations of the evolution of an initial condition perturbed a small amount from a saddle by the unstable eigenvector, I determined numerically that $\left|\rho_c - 3/\sqrt{2}\right| < 10^{-14}$. However, I have not been able to rigorously show that $\rho_c = 3/\sqrt{2}$. It is also interesting that this predicted value occurs when the square defined by the equilibria has an edge of length $\pi/2$, which is the mean of the length the cases when $\rho = 0$ and the case when $\rho = 3$.

Different Intrinsic Frequencies

Let us now break the symmetry of the system and change the intrinsic frequencies of the two end oscillators so that they are slightly different. The mean of the intrinsic frequencies of these two oscillators is $\bar{\omega} = (\omega_1 + \omega_3)/2$, and their scaled difference (as a fraction of the coupling strength) is $\epsilon \equiv (\omega_1 - \omega_3)/2K$. Because $\omega_1 \neq \omega_3$, we define $\rho \equiv (\omega_2 - \bar{\omega})/K$. Equation (3) becomes

$$\begin{aligned} \dot{\phi}_1 &= \rho - \epsilon - 2\sin\phi_1 - \sin\phi_2, \\ \dot{\phi}_2 &= \rho + \epsilon - 2\sin\phi_2 - \sin\phi_1. \end{aligned} \tag{4}$$

There exists equilibrium points provided $|\rho - 3\epsilon| < 3$. The square of equilibria is now a rectangle whose aspect ratio increases as ϵ increases from 0. However, the directions of the eigenvectors are invariant of ϵ. The system's global

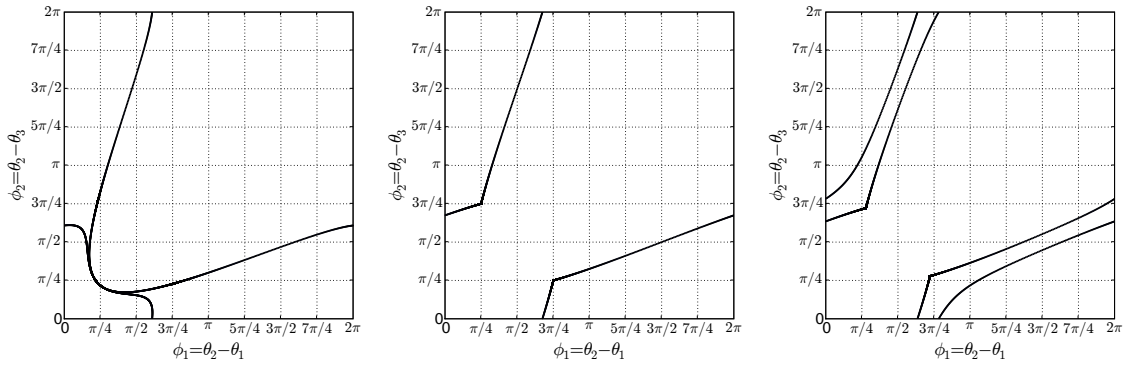

no closed orbits $\rho < 3/\sqrt{2}$ | heteroclinic orbit $\rho = 3/\sqrt{2}$ | homoclinic orbits $3/\sqrt{2} < \rho < 3$

FIG. 2: The phase space of equation (3) will either have a basin of attraction to the stable equilibrium point or not depending on the unstable manifolds of the saddles .The three cases for the unstable manifolds of the saddles of equation (3) are: the unstable manifold connects to the stable manifold of the stable equilibrium, the center unstable manifold connects to the stable manifold of the other saddle, and the right unstable manifold connects to the stable manifold of the same saddle.

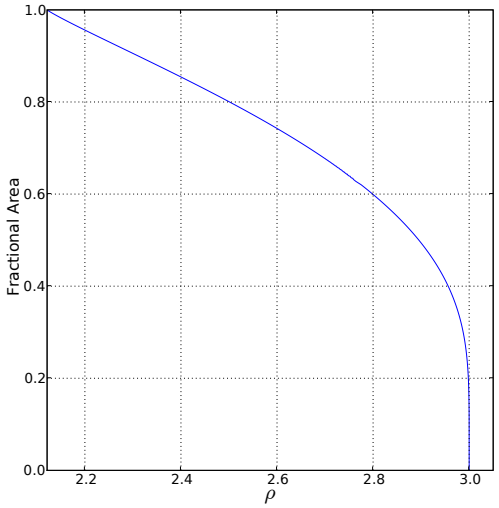

FIG. 3: Area of basin of attraction of (3) as a fraction of the entire space. Note the constant slope as $\rho \to \rho_c$ and sudden drop as $\rho \to 3$.

dynamics experience an important change, as homoclinic orbits are not possible for $\epsilon \neq 0$. This implies there is not a separatrix, so the basin of attraction of the stable equilibrium extends to the entire phase space. This is remarkable as it suggests that it is easier to synchronize oscillators when the intrinsic frequencies are *different* rather than when they are the same. Instead of a region in phase space where initial conditions can not reach the stable equilibrium, there is now a region where initial conditions reach the stable equilibrium very slowly for small enough ϵ (see Fig. 4).

Because homoclinic orbits only occur for $\epsilon = 0$, it would seem there is something special about the symmetric case in which the intrinsic frequencies of the two end oscillators the same. It seems that this is supported by the fact that the phase portrait of (3) is symmetric across $\phi_1 = \phi_2$

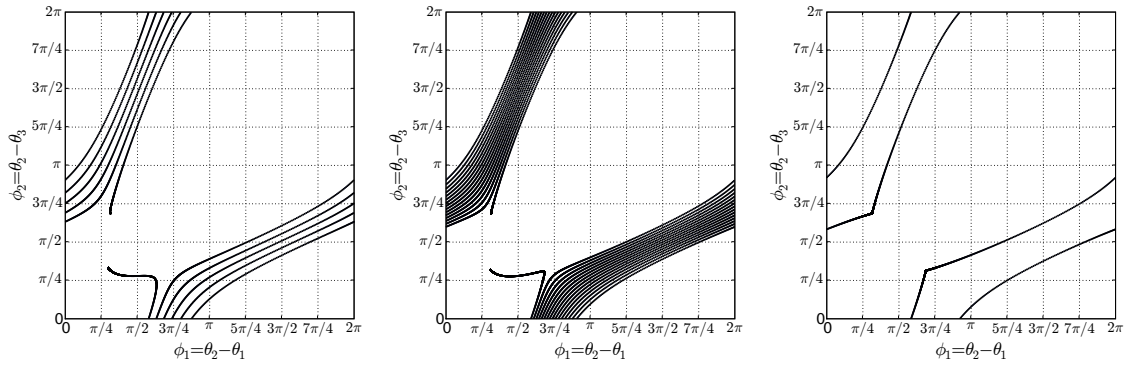

$\epsilon = 0.03$ $\epsilon = 0.01$ $\epsilon = 0$

FIG. 4: Unstable manifold of saddle labeled (B) in Fig. 1 for the dynamical system (4) with $\rho = 5/2$. The unstable manifold winds around phase space many times (relative to other trajectories) before it comes to rest at the stable equilibrium. As $\epsilon \to 0$, the orbit becomes more dense, the homoclinic orbit of system (3) is recovered, and one obtains a separatrix (inside of which are infinitely many cycles [not pictured]).

All-To-All Coupling

The dynamics for three oscillators that are all coupled to each other markedly different. The dynamical equations for relative phases now have an additional term to describe the coupling between θ_1 and θ_3. When the intrinsic frequencies of two of the oscillators are the same, the equations of motion are given by

$$\begin{aligned} \dot{\phi}_1 &= \rho - 2\sin\phi_1 - \sin\phi_2 - \sin(\phi_1 - \phi_2), \\ \dot{\phi}_2 &= \rho - 2\sin\phi_2 - \sin\phi_1 - \sin(\phi_2 - \phi_1). \end{aligned} \tag{5}$$

This system can now have as many as 6 equilibria, but only one of them is stable. As before the stable equilibrium is located at $(\arcsin(\rho/3), \arcsin(\rho/3))$. Similar to the the case of the line topology a bifurcation occurs at $\rho = 3$. No equilibria exist for $\rho > 3$. For $3/4 < \rho < 3$, there are only two equilibria: the aforementioned stable node and a saddle. For these values of ρ, all initial conditions are drawn to the stable equilibrium and synchronize. A saddle-node bifurcation occurs at $\rho = 3/4$ (see Fig. 5). When $0 < \rho < 3/4$, the system has 4 additional equilibria, (two saddle-source pairs). Because only one of the equilibria is stable, all initial conditions synchronize as long as the space is not separated by homoclinic or heteroclinic orbits. By creating trapping regions based on the nullclines (curves defined when either ϕ_1 or ϕ_2 vanish), one can see that such orbits are not possible for this system. Therefore all initial conditions are drawn to the stable equilibrium.

PHASE-AMPLITUDE MODEL

For most applications, it is much more realistic to include both amplitude as well as phase. The following model is directly applicable to nano-electromechanical systems (NEMS) and arrays of lasers coupled together to increase power output:

$$\dot{z}_n = i(\omega_n - \alpha\,|z_n|^2)z_n + (1 - |z_n|^2)z_n + i\sum_{m=1}^{N} \beta_{n,m}\,(z_m - z_n)\,. \tag{6}$$

Here $z_n = r_n e^{i\theta_n}$ describes both an amplitude and a phase. Equation (6) has a coupling constant β that is imaginary, which is *reactive*, in contrast to the dissipative coupling of models such as (1). This is known to be a "reactive" coupling, because when this equation is derived from a *van der Pol-Duffing* oscillator, a coupling through position, rather than velocity gives rise to an imaginary term. Coupling through position is referred to as reactive because the

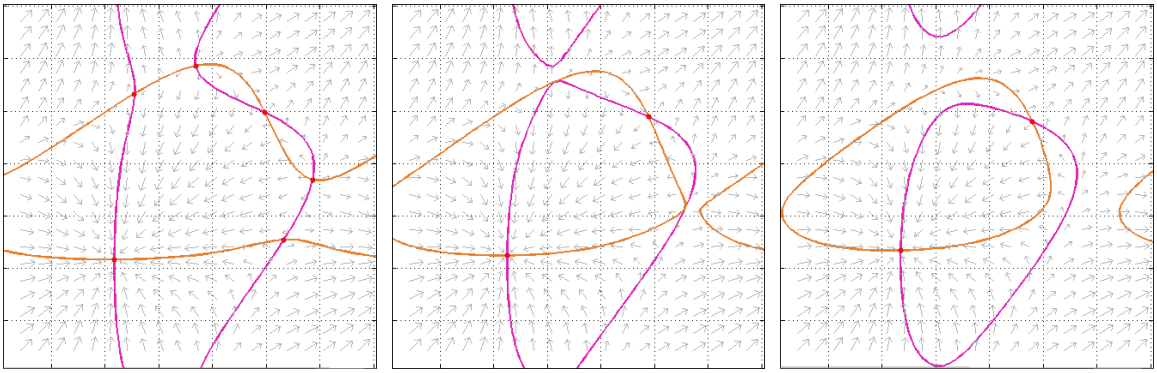

FIG. 5: Phase portraits for the dynamical system (5). The axes are ϕ_1 and ϕ_2. Equilibrium points and nullclines are drawn. The horizontal axes are ϕ_1 and the vertical axes are ϕ_2. The saddle-node bifurcation is shown at $\rho = 3/4$. The nullclines indicate that homoclinic orbits cannot occur.

sign of the term does not change when time is reversed [3]. This model also contains a term that makes the frequency dependent on amplitude (this is known as frequency pulling).

Consider the case $N = 2$. We first check that "amplitude death" does not occur. That is, the solution $z_n = 0$ for all n is stable, leading to the collapse of the amplitudes of the oscillators. In [4], Jeff Rogers showed that amplitude death occurs for some range of the parameters for $N = 3$ with dissipative coupling when $\alpha = 0$. By examining the Jacobian for two oscillators, I found that the eigenvalues of the amplitudes always have a real part equal to $+1$, so that the solution at the origin is unstable for all parameter values.

When $N = 2$, equation (6) can be rewritten as a system of three equations - two amplitudes and one phase difference $\phi \equiv \theta_2 - \theta_1$.Defining$\Delta\omega \equiv \omega_2 - \omega_1$, the equations of motion are written as

$$\begin{aligned} \dot{r}_1 &= \left(1 - r_1^2\right) r_1 - \beta r_2 \sin\phi, \\ \dot{r}_2 &= \left(1 - r_2^2\right) r_2 - \beta r_1 \sin\phi, \\ \dot{\phi} &= \Delta\omega - \alpha\left(r_2^2 - r_1^2\right) - \beta\left(\frac{r_2}{r_1} - \frac{r_1}{r_2}\right)\cos\phi. \end{aligned} \tag{7}$$

In this case, synchronized solutions consist of equilibrium points; They have constant amplitude and are frequency locked. Numerical root finding shows that there is at least one equilibrium for all ranges of parameters and that some ranges include two equilibria.

One can determine conditions for which synchronization cannot occur by finding parameter values such that the synchronized equilibrium point has at least one positive eigenvalue. To find such a bound, I restricted the amplitudes to curves where the equilibria exist and computed which parameter values yielded an instability. This results in two curves in parameter space (one for each of the two solutions):

$$\beta(\Delta\omega) = \sqrt{\frac{1}{8}\left(1 + 3\alpha^2 \pm 4\sqrt{3}\alpha\Delta\omega + 4\Delta\omega^2\right)}. \tag{8}$$

As shown in Fig. 6, the curves (8) are fairly good at predicting where synchronization occurs. The numerical simulations verify the calculations of the curves. I plotted the curves in the $\Delta\omega$ - β plane; changing α causes the bottom curve to shift to the right and the top curve to shift to the left.

To examine the two solutions, I made various sweeps of the parameters to try to find solution branches (see Fig. 7 for an example). These diagrams show expected behavior such as multiple solution branches and (to a small extent) hysteresis, as well as some unexpected and strange behavior. In the unsynchronized region there appear gaps, with arcs passing through that look almost like synchronized solutions. However, simulations at these points show that the oscillators are not synchronized. When the system is not synchronized the order parameter will oscillate. This behavior might be expected to occur when the length of the simulation is a near integer multiple of the primary period of oscillation. One could test this using a series of sweeps with a random step size.

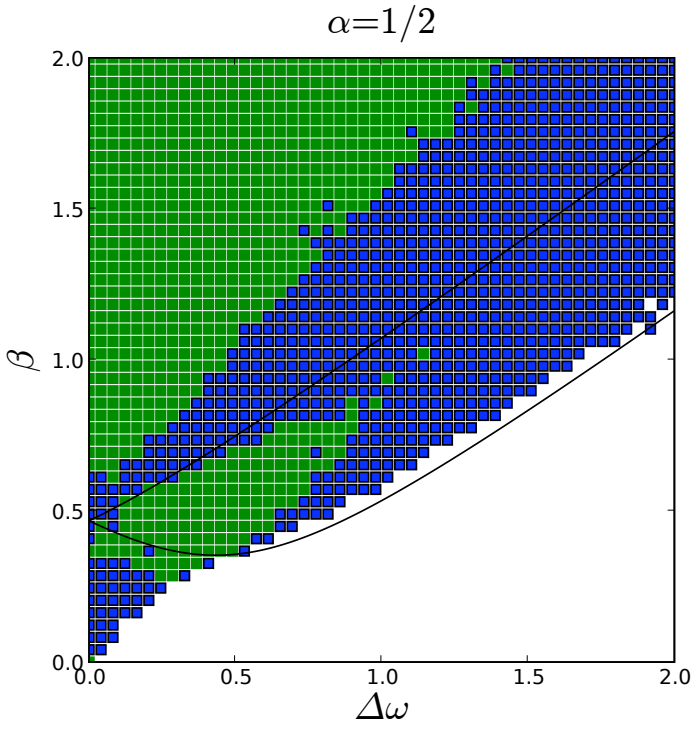

FIG. 6: [Color online] Synchronization in the dynamical system (6) for different regions of parameter space. Each point encompasses 25 simulations with initial phases selected uniformly from all values and initial amplitude selected uniformly at random from [0,1]. Green (light) dots are parameter values in which all 25 runs synchronized after a set time. Consider synchronization to have occurred for a given parameter pair the order parameter $|z_1 + z_2|/2$ settles to a constant value (within some tolerance). The blue (dark) dots are those parameters in which at least one zero run synchronized. The white spaces are parameter values that never synchronized. The two black curves were calculated in equation (8) to be the stability boundaries.

CONCLUSIONS

In this paper I classified the dynamics of coupled systems of three phase oscillators with different intrinsic frequencies and coupling topologies but with equal coupling strengths. I verified the results using numerical simulation. I found that the symmetric case of the phase model (i.e two equal intrinsic frequencies) exhibits unexpected dynamics behavior as it contains an interval of parameters values with a region of initial conditions cannot synchronize. This arises because the homoclinic orbits of the saddles in phase space create a basin of attraction. When the symmetry is broken this region becomes a region in which trajectories pass though slowly.

I plan to extend this work be determining a more precise description of the global bifurcations that occur in the phase model with symmetrical frequencies [see equation (3)]. A more rigorous explanation of why homoclinic orbits form is desirable, and $\rho_c = 3/\sqrt{2}$ requires exact verification.I obtained some results for a system of two oscillators with nonlinear frequency pulling. This system exhibits a lot of rich behavior, such as a lack of amplitude death, and it includes multiple stable solutions and hysteresis. More work must be done to describe the region of synchronization that lies below the first solutions bound of stability, where synchronized solutions have been calculated to be unstable (see Fig. 6). Once a solid understanding of the two oscillator system is achieved I will examine a system three oscillators with amplitudes, studying first a line topology with identical intrinsic frequencies on each end.

Appendix: Stability Bounds

As with the phase equation, the amplitude equations (6) can be simplified using a relative phase $\phi \equiv \theta_2 - \theta_1$:

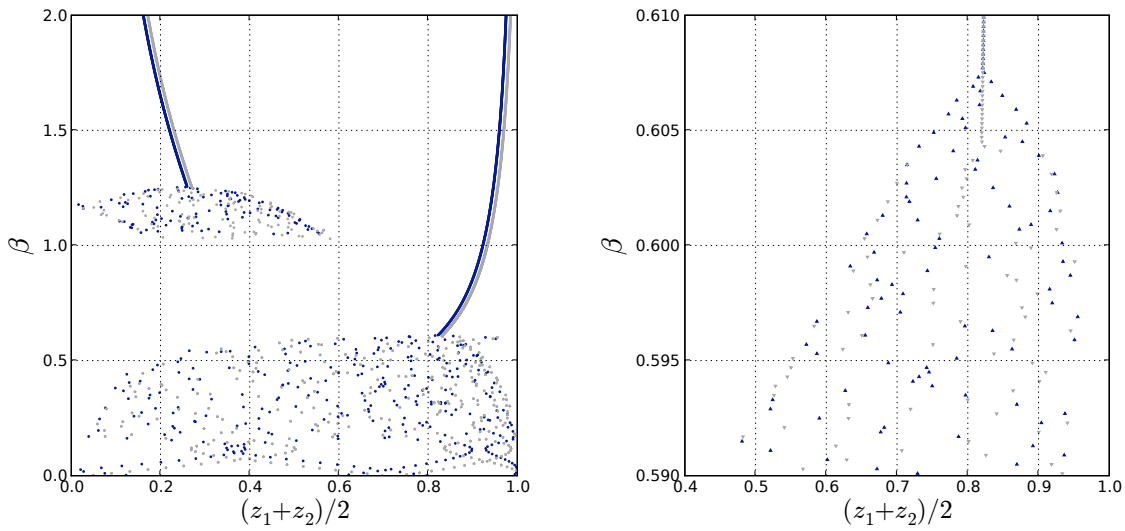

FIG. 7: [Color online] Sweep of parameter β for equation (6) with $\alpha = 1/2$ and $\Delta\omega = 1$. The blue (dark) dots are sweeps from 0 to 2, and the gray (light) dots are sweeps from 2 to 0. One can clearly see that there are two stable solutions can be clearly seen. The scattered dots are unsynchronized solutions, in which the average amplitude is oscillating at the end of the simulation, and the solid curves are synchronized solutions, for which the average amplitude settles to a constant value. One can see two regions for which an unsynchronized solution is stable. There is also a region of bistability ($\beta \sim$ [1.05,1.25]). To stay on a solution branch, I ran a simulation for some time, and the final conditions of the simulations would were used for the next simulation's initial conditions (after the parameter was gradually adjusted). Hysteresis occurs in the bistable region.

$$\begin{aligned} \dot{r_1} &= (1-r_1^2)r_1 - \beta r_2 \sin\phi, \\ \dot{r_2} &= (1-r_2^2)r_2 + \beta r_1 \sin\phi, \\ \dot{\phi} &= \omega_2 - \omega_1 - \alpha(r_2^2 - r_1^2) + \beta\left(\frac{r_1}{r_2} - \frac{r_2}{r_1}\right)\cos\phi. \end{aligned} \tag{9}$$

This manipulation is desirable because the equilibria are synchronized points (I assume synchronized states will have constant amplitude because numerically that is all I see). Setting $\dot{r_1} = \dot{r_2} = 0$ yields:

$$r_1^2 - r_2^2 + r_2^4 - r_2^2 \tag{10}$$

This is a curve in the $(r_1, r_2)-$plane on which all synchronized solutions must lie. By restricting to this curve and assuming a solution exists (this can be checked numerically), the stability of solutions along this curve can be tested by examining the Jacobian of the amplitude equations of (9):

$$\begin{pmatrix} 1-3r_1^2 & -\beta\sin\phi \\ \beta\sin\phi & 1-3r_2^2 \end{pmatrix} \tag{11}$$

This yields the characteristic equation.

$$(1-3r_1^2-\lambda)(1-3r_2^2-\lambda) + \beta^2\sin^2\phi = 0. \tag{12}$$

Substitute in $(1-r_1^2)r1/r2 = \beta\sin\phi$ from (9):

$$(1-3r_1^2-\lambda)(1-3r_2^2-\lambda)r_2^2 + (1-r_1^2)^2 r_1^2 = 0 \tag{13}$$

Using (10) I show that $r_1 > \sqrt{3+\sqrt{3}/2}$ and $r_2 > \sqrt{3-\sqrt{3}/2}$.

Inserting thisinto (9) gives a condition on the value of β in terms of the frequency difference $\Delta\omega$ and frequency pulling term α:

$$\beta(\Delta\omega) = \sqrt{\frac{1}{8}\left(1 + 3\alpha^2 \pm 4\sqrt{3}\alpha\Delta\omega + 4\Delta\omega^2\right)} \tag{14}$$

Acknowledgments

I gratefully acknowledge my mentors Mike Cross and Mason Porter for their direction and oversight. I would also like to thank Oleg Kogan for many invaluable discussions, Jeff Rogers for his assistance and advice concerning numerical simulations, Ron Lifshitz, and the other students in the group for their assistance in revising papers and the constructive research environment they provided. This research opportunity was made possibly by funds from the Caltech's Summer Undergraduate Research Fellowship (SURF) program and from Boeing.

[1] Juan A. Acebron, L. L. Bonilla, Conrad J. Perez Vicente, Felix Ritort, and Renato Spigler. The Kuramoto model: A simple paradigm for synchronization phenomena. *Reviews of Modern Physics*, 77, 2005.

[2] J. Buck and E. Buck. *Synchronous fireflies.* Scientific American, 1974.

[3] Michael C. Cross, Jeffrey L. Rogers, Ron Lifshitz, and Alex Zumdieck. Synchronization by reactive coupling and nonlinear frequency pulling. *Physical Review E*, 73, 2006.

[4] Jeffrey L. Rogers. Analysis of three coupled limit-cycle oscillators. Preprint, 2007.

[5] Steven Strogatz. From Kuramoto to Crawford: Exploring the onset of synchronization in populations of coupled oscillators. *Physica D*, 143, 2000.

[6] Steven H. Strogatz. *Sync: The Emerging Science of Spontaneous Order.* Hyperion, 2003.